SANDIA REPORT
SAND2014-0588
Unlimited Release
Printed January 2014

Micro-Scale Heat-Exchangers for Joule-Thomson Cooling

Andrew Gross

Prepared by
Sandia National Laboratories
Albuquerque, New Mexico 87185 and Livermore, California 94550

Sandia National Laboratories is a multi-program laboratory managed and operated by Sandia Corporation, a wholly owned subsidiary of Lockheed Martin Corporation, for the U.S. Department of Energy's National Nuclear Security Administration under contract DE-AC04-94AL85000.

Sandia National Laboratories

Issued by Sandia National Laboratories, operated for the United States Department of Energy by Sandia Corporation.

Available to DOE and DOE contractors from
U.S. Department of Energy
Office of Scientific and Technical Information
P.O. Box 62
Oak Ridge, TN 37831

Telephone:	(865) 576-8401
Facsimile:	(865) 576-5728
E-Mail:	reports@adonis.osti.gov
Online ordering:	http://www.osti.gov/bridge

Available to the public from
U.S. Department of Commerce
National Technical Information Service
5285 Port Royal Rd.
Springfield, VA 22161

Telephone:	(800) 553-6847
Facsimile:	(703) 605-6900
E-Mail:	orders@ntis.fedworld.gov
Online order:	http://www.ntis.gov/help/ordermethods.asp?loc=7-4-0#online

SAND2014-0588
Unlimited Release
Printed January 2014

Micro-Scale Heat-Exchangers for Joule-Thomson Cooling

Andrew Gross
Department Names
Sandia National Laboratories
P.O. Box 5800
Albuquerque, New Mexico 87185-MS1084

Abstract

This project focused on developing a micro-scale counter flow heat exchangers for Joule-Thomson cooling with the potential for both chip and wafer scale integration. This project is differentiated from previous work by focusing on planar, thin film micromachining instead of bulk materials. A process will be developed for fabricating all the devices mentioned above, allowing for highly integrated micro heat exchangers. The use of thin film dielectrics provides thermal isolation, increasing efficiency of the coolers compared to designs based on bulk materials, and it will allow for wafer-scale fabrication and integration. The process is intended to implement a CFHX as part of a Joule-Thomson cooling system for applications with heat loads less than 1mW. This report presents simulation results and investigation of a fabrication process for such devices.

.

ACKNOWLEDGEMENTS

1) This work was funded under LDRD Project Number158181 and Title "Micro-scale Heat Exchangers for Cryogenic Micro-cooling Applications"

CONTENTS

FIGURES

TABLES

Nomenclature

DOE	Department of Energy
SNL	Sandia National Laboratories
J-T	Joule-Thomson
CFHX	Counter Flow Heat Exchanger
CDE	Chemical Downstream Etcher
RIE	Reactive Ion Etcher
DRIE	Deep Reactive Ion Etcher
ICP	Inductively Coupled Plasma
LPCVD	Low Pressure Chemical Vapor Deposition

1. INTRODUCTION

The purpose of this project was to evaluate the possibility of using truly micro-scale heat exchangers to enable on-chip localized cryogenic cooling of high-performance micro-scale sensors, actuators and electronics. There many types of devices that can benefit from low temperature operation. Devices such as bolometers see an increase in sensitivity, due to reduced noise when operated at low temperatures. Low noise amplifiers also see a reduction in thermal noise when operated at low temperatures, which is useful in achieving high signal to noise ratios. In addition, resonant MEMS devices such as gyroscopes, resonators and filters have all been shown to demonstrate increases in the quality factor with reduced temperatures. Achieving such increases in Q allows for higher performance rotational sensing, higher quality frequency sources and better filters.

Currently, cooling of such micro-scale devices to temperatures below ambient is often done with meso, or even macro-scale systems. Thermo-electric systems have been demonstrated to provide minimum temperatures of as low as 180K [1], however they require significant amounts of power to achieve that level of cooling. In addition, high performance thermoelectric coolers rely on materials systems, such as Bismuth telluride, antimony telluride, or epitaxially grown super-lattice structures that present significant challenges for integration with typical MEMs and micro-electronic fabrication process. As a result the thermo-electric cooling is implemented in a separate module that is then attached to the device being cooled. The effect of such an integration scheme is that the device being cooler must be fabricated separately from any control and interface circuits, or the cooler must have the capacity to cool both the intended device as well as the rest of the system. Other forms of low temperature cooling suffer from the same problems. Meso-scale Joule-Thomson coolers have been produced with the intention of integration with MEMS and micro-electronic devices [2-6]. These coolers have reached temperatures as low 100K. However, the solutions demonstrated to date do not adequately address system integration and packaging. This project investigated the possibility of creating micro-scale coolers on chip, with the capability to cool a target device below 200K. An open system using the Joule-Thomson effect was investigated. The key structure for this type of cooler, is a counter-flow heat exchanger, in which a hot fluid moving in one direction is able to exchange heat with a cooler fluid moving in the opposite direction without mixing of the two fluids.

The remainder of this report will present work done on both modeling and fabrication related to building a micro-scale counter-flow heat exchanger and Joule-Thomson cooler. A proposed fabrication process for building a micro-scale counter flow heat exchanger is outlined, and results of fabrication short-loops are presented. The results of these short-loops revealed unexpected obstacles which will be discussed below. Modeling of the counter-flow heat exchanger, a gas expansion orifice and a complete Joule-Thomson cooler is presented, and the results of this modeling are used to propose a future direction for additional development.

2. INITIAL COUNTER FLOW HEAT EXCHANGER MODELING

2.1 Introduction

The Joule-Thomson effect occurs when a real gas under high-pressure is expanded through an orifice or restriction under isenthalpic conditions. The expansion is adiabatic and the gas does no work during the expansion. The temperature will either rise or fall, depending the gas being used and the initial temperature of the gas prior to expansion. For nitrogen, cooling occurs for starting temperatures below 621K, while helium will heat when expanded at temperatures 51K. The Joule-Thomson coefficient specifies the temperature change per pressure change. Even at high pressures this only results in total temperature change of a few tens of degrees. To make an effective cooler using the J-T effect a counter-flow heat exchanger is need. In this system the high-pressure gas begins at room temperature. As it expands it cools, and the cooled, low pressure gas returns along a path that allows it to exchange heat with the warmer high pressure flow. This creates a positive feedback loop that can gradually drop the temperature of the expanded gas to the liquefaction point.

The key to creating a micro-scale Joule-Thomson cooler is the fabrication of the counter-flow heat exchanger. Previous work on small scale Joule-Thomson coolers has resulted in devices that relied on complex stacks of wafers that used thick bulk materials[2,3,5,6]] or were not compatible with planar processing techniques[4]. The CFHX envisioned for this project would consisted of co-axial tubes, having silicon nitride walls as shown in Figure 1. The first step in designing a cooler around such a structure was to verify through modeling, that the necessary heat transfer between the high pressure and low pressure gas flows could occur given different wall and gas parameters. The initial modeling of the counter-flow heat exchanger was performed using a custom code written in python. The goal of this phase of the project was to create a tool capable of fast simulation of the counter flow heat exchanger, under a set of simplifying assumptions.

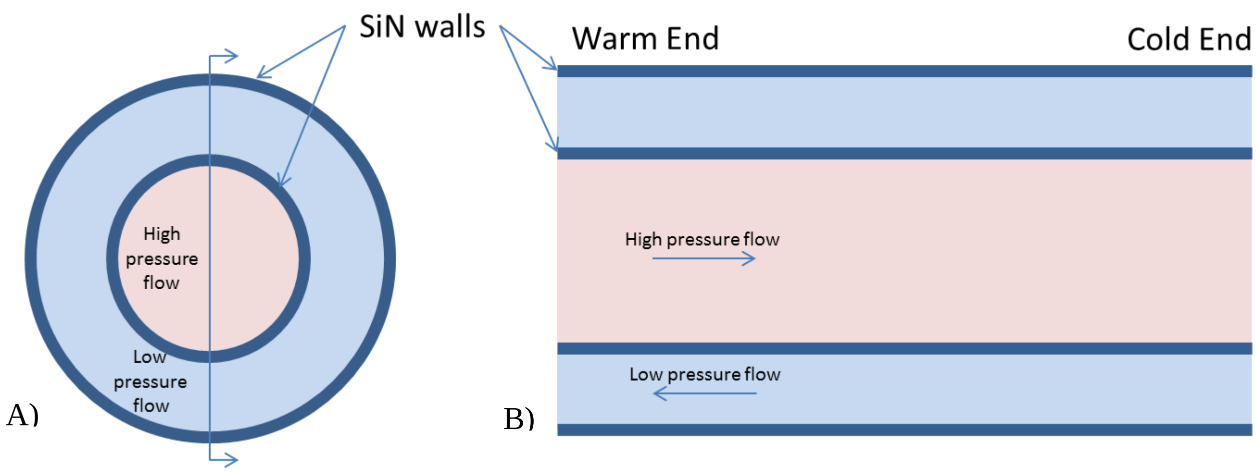

Figure 1: Transverse and Longitudinal cross-sections of an idealized co-axial counter flow heat exchanger.

2.2 Convection-Diffusion Equation Discretization

To model a co-axial counter flow heat exchanger the convection-diffusion PDE was used:

$$\rho C_p \frac{dT}{dt} = -\vec{v} \cdot \nabla \left(\rho C_p T\right) + \nabla \cdot (-k\nabla T) + s \qquad [1]$$

where ρ is the density of the material, T is temperature in Kelvin, υ is velocity k is thermal conductivity, C_p is the material heat capacity at constant pressure, and the s represents a heat source/sink in W/m^2. Discretizing equation 1 using a first order finite differencing at steady state yields (dT/dt=0) on a rectangular grid in a 2-D axially symmetric system as shown in Figure 2. results in equation 2 for a point (i,j):

$$-w_{in_{i,j}} = v_{i_{i,j,}} \rho_{i,j} C_{p_{i,j}}\, 2\pi R_{i,j} \Delta r\, \left[T_{i,j-1} - T_{i,j}\right] + \left[K_{j+}\left[T_{i,j+1} - T_{i,j}\right] - K_{j-}\left[T_{i,j} - T_{i,j-1}\right]\right] + \left[K_{i+}\left[T_{i+1,j} - T_{i,j}\right] - K_{i-}\left[T_{i,j} - T_{i-1,j}\right]\right] \qquad [2]$$

where i and j are integers indicating the radial and axial position respectively. w_{in} is the total heat dissipated in the volume associated with point (i,j), and K_{j+} is the total thermal conductance from point (i,j) to point (i,j+1) and is calculated for each point to include both geometric and material variations. K_{j-}, K_{i+}, K_{i-} have a similar interpretation. The velocity is restricted to a vector parallel to axis of symmetry. When applied to a physical system, equation 2 is used to generate a system of linear equations that can be represented as a sparse matrix, and the temperature at each point can be calculated.

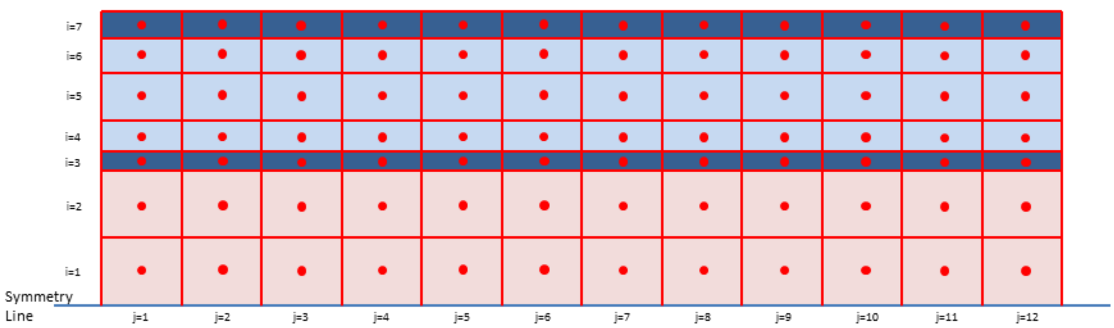

Figure 2: Schematic representation of the finite difference discretization scheme used for the convection-diffusion model. Red dots represent the locations of the discretized points. The red rectangle surrounding the dot is the real area that the point represents in the model.

2.3 Results

To implement a model based on the above discretization, a number of assumptions were used. First, it was assumed that the pressure along the length of the pipe was negligible compared to the drop across the restriction. This allowed the pressure to be modeled as constant along the length of the high-pressure and low pressure flows. Second, it was assumed that all flow was laminar, fully developed pipe-flow with a no slip boundary condition. This allowed the velocity to be calculated analytically. The restriction and the isenthalpic expansion were accounted for as a negative heat source attached to the cold end of the heat-exchanger. The magnitude of the heat removal was determined but the change in total enthalpy of the gas between the high-pressure and low-pressure sides, at a given temperature. The total enthalpy was calculated using the mass-flow rate combined with material properties for nitrogen published by NIST [9].

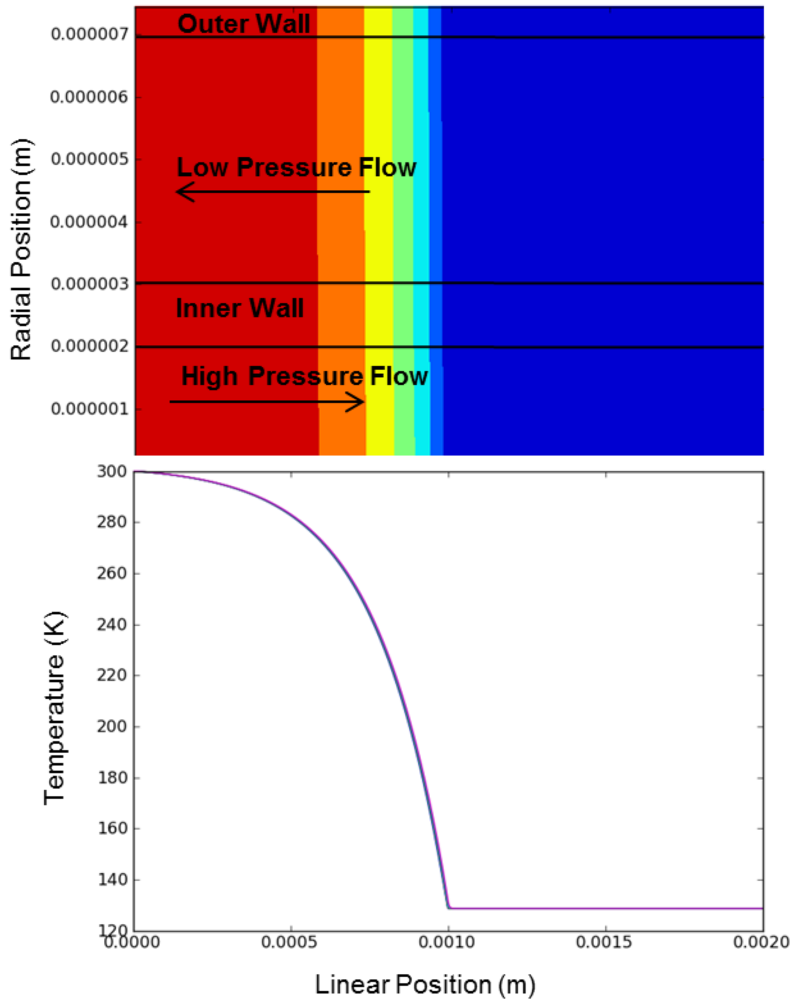

Figure 3. Simulation results of a 1mm long CFHX with a 1um thick SiN inner wall, and 0.5um thick outter wall, with an 80atm pressure differential between the high and low pressure flows (x and y scales are not the same). The top plot shows temperature contours in the axis-symmetric cross section, while the bottom plot shows temperature vs linear position along the symmetry axis.

Results of this simulation effort showed that good heat transfer between the high low pressure flows could be achieved. This can be seen in Figure 3. by the fact that the two flows are have very little difference in temperature at any given position. These simulations gave a strong indication that a structure of co-axial SiN tubes could be an effective counter-flow heat exchanger, but as more detailed solutions were pursued it became clear that the code was note able to produce accurate predictions exact temperature and cooling power. The weakness in code as written, was an inability to handle the non-linear dependence of the heat capacity on temperature, which varies along the length of the CFHX. Incorporating this dependency into the discrete model resulted in a set of non-linear equations that require significantly more complex solution algorithms. As a result, this model was tabled in favor of commercial finite element tools.

3. FABRICATION

3.1 Proposed Process

The concept of the creating dielectric tubes for micro-fluidic has been previously investigated [7,8], and this work builds on those processes to explore the possibility of fabricating co-axial tubing for a heat exchanger applications. The initially proposed process for the fabricating the co-axial silicon nitride tubes is shown in Figure 4. The basic fabrication steps are as follows (details provide later in this section:

1) Perform a DRIE etch in a silicon wafer to define trenches.
2) Protect the sidewalls of the trenches.
3) Perform a dry isotropic silicon etch to create a tube-like profile. (Figure 4a)
4) Deposit SiN to create a tube wall and seal the trench. (Figure 4b)
5) Open trenches in the SiN adjacent to the original silicon trench using RIE.
6) Perform a dry isotropic silicon etch to remove the silicon around first tube. (Figure 4c)
7) Deposit SiN to create a tube wall on the outer tube, and seal the openings to the surface. (Figure 4c)

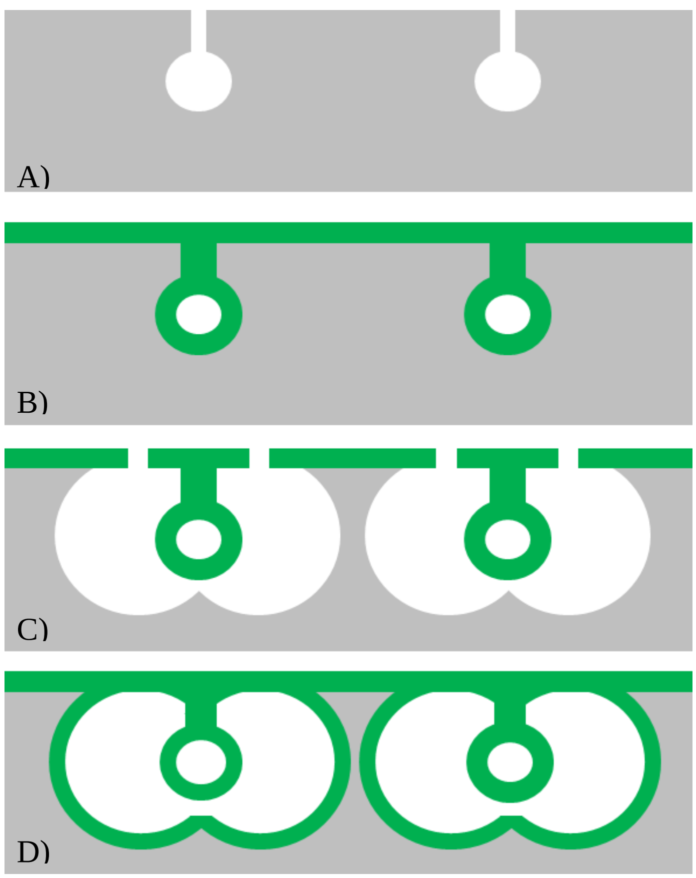

Figure 4: Conceptual process flow for co-axial tubing. A) DRIE is used to create a trench in Si, and an isotropic silicon etch is used to expand the bottom of the hole. B) conformal LPCVD nitride is use to coat the inside of the hold and seal the trench. C) the SiN is etched to the silicon adjacent to the first pipe, and an isotropic silicon etch is used to open a cavity surrounding the tube. D) A second deposition of LPCVD SiN is used to create the walls of the outter tube and to seal the openings.

3.2 Fabrication Results

A mask was design to fabricate trenches ranging from 1um wide to 5um wide. The wafers were first coated with 1um of oxide, which was then etch and used as a hard mask for the subsequent DRIE etch. Wafers were split at the trench etch to target either 5um or 10um depth in the 3um wide trenches. Follow the DRIE the wafers were further split to protect the side wall of the trench with native DRIE polymer or 1000A of oxide. In the case of the wafers receiving the oxide an additional RIE step was performed to remove the oxide from the bottom of the trench. The wafers were then etch in Chemical Downstream Etching (CDE) system using NF3 and Ar. Resulting etch profiles for the 3um wide trenches are shown in Figure 5 and Figure 6. Figure 6 shows that although it provided some level of protection, the DRIE polymer was not robust enough to serve as an etch stop on the sidewall of the trench. In all cases the etch profile was not as isotropic as desired and demonstrate a directional dependency.

Figure 5: Cross-sections of channels formed using CDE etching after trench formation. The side walls were protected with 1000A of LPCVD oxide. A) Using a 3um wide trech that was originally 5um deep. B) Using 3um wide trech that was originally 10um deep.

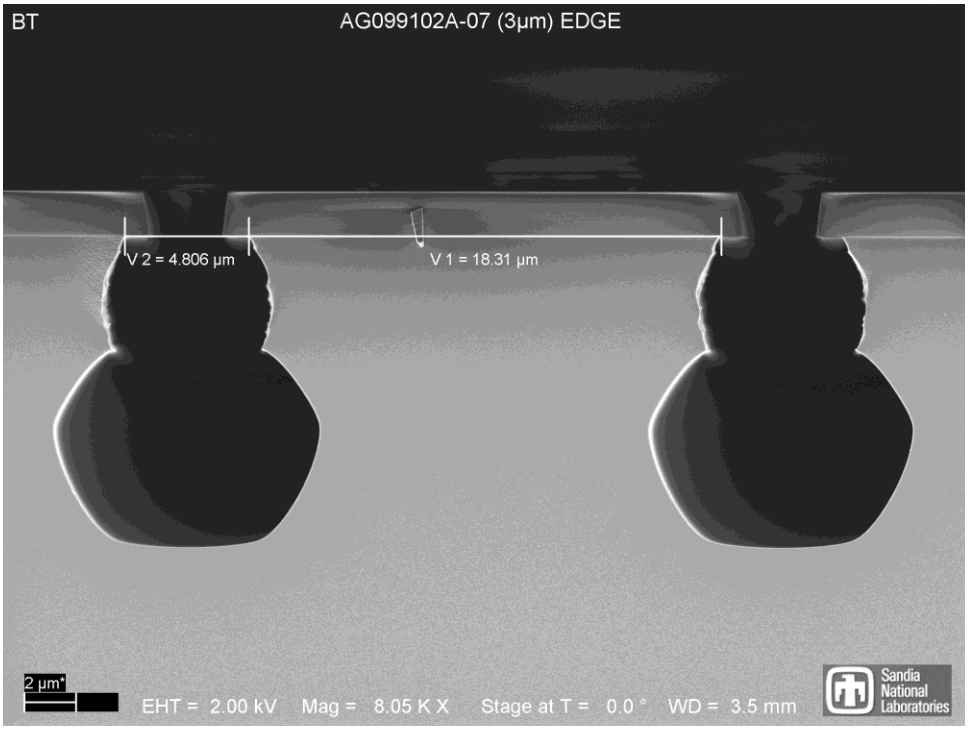

Figure 6: Cross-section of a test to use the DRIE polymer to protect the trench side-walls during CDE etching. The polymer failed during the etch, causing an undesirable profile.

After the CDE etch the wafers were coated with SiN in an LPCVD process, and then capped with LPCVD SiO2. Cross-sections obtained following these depositions are shown in Figure 7. and Figure 8 for the case of a 5um deep trench and a 10um deep trench respectively. The profile obtained for the sub-surface tube was similar in both cases, but presented two significant problems. First, the top of the trench sealed before the bottom of the trench, resulting in a long open seam in the trench. When pressurized this would result in significant stress, and would likely cause the structure to fail. Second, the LPCVD depositions caused exaggeration of the interior corners; this is particularly evident on the larger structures with thicker depositions. These sharp corners would also act as significant stress concentrators, and as simulations shown later indicate, they would also result in device failure at high pressures.

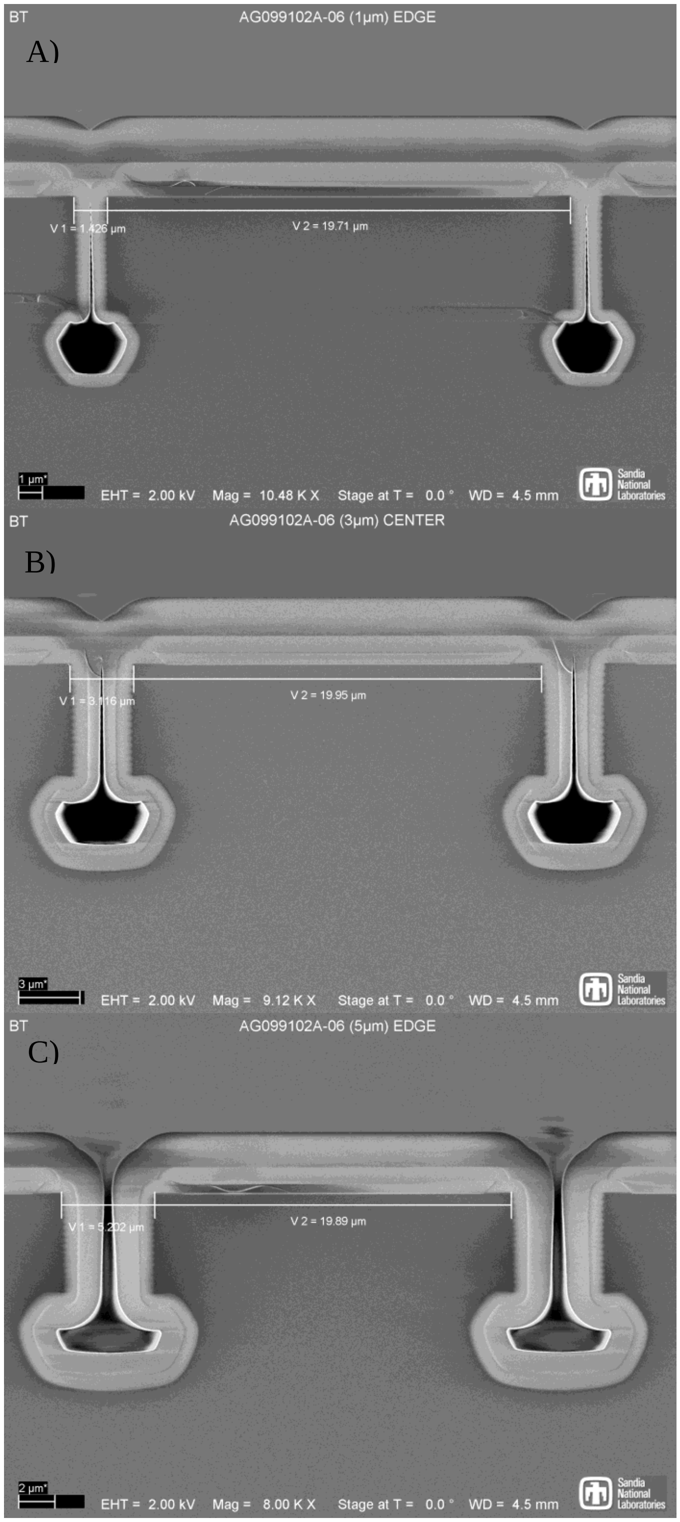

Figure 7: Cross-sections of sub-surface tubes after resealing with dielectric. Note the sharp corners and long seam present in all cases. The profiles were formed by starting with A) a 1um x 5um (width x height) trench, B) a 3um x 5 um trench, and C) a 5 um x 5um trench.

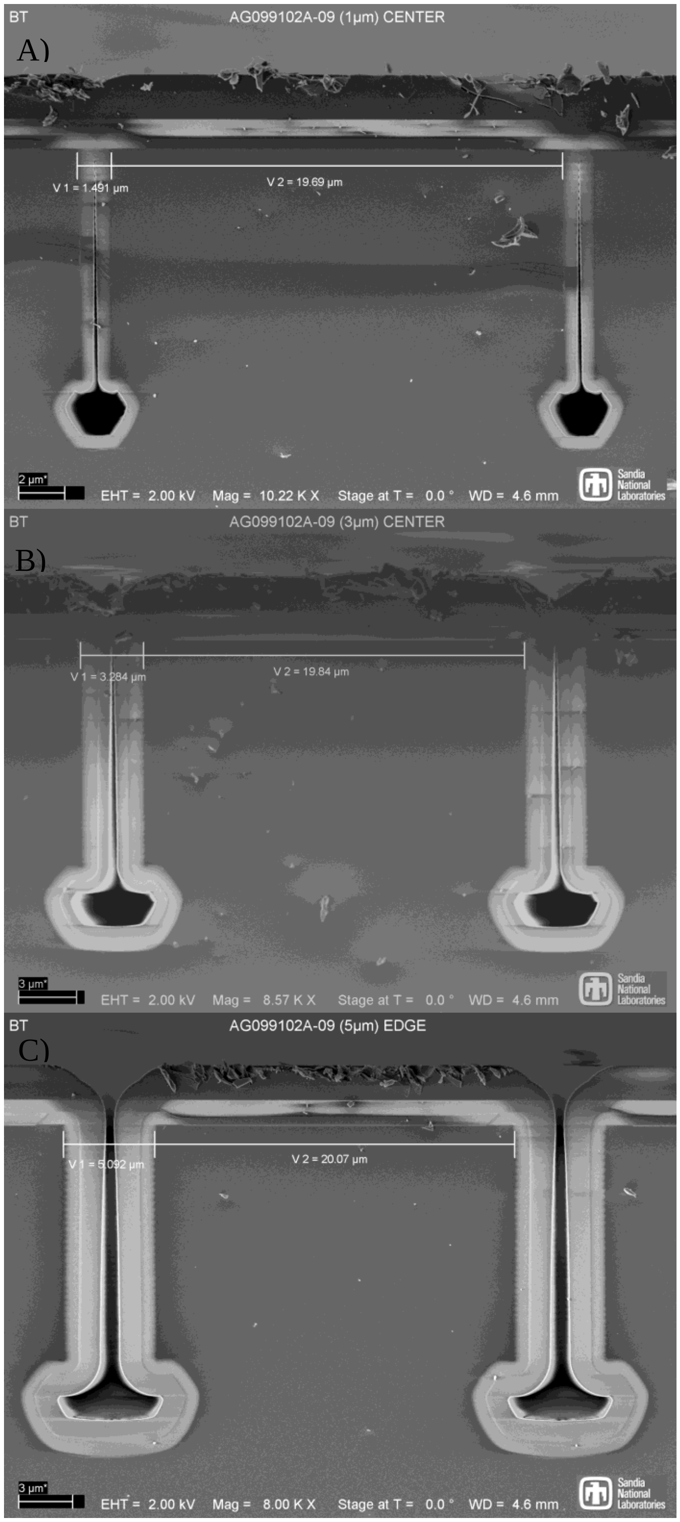

Figure 8: Cross-sections of sub-surface tubes after resealing with dielectric. Note the sharp corners and long seam present in all cases. The profiles were formed by starting with A) a 1um x 10um (width x height) trench, B) a 3um x 10 um trench, and C) a 5 um x 10um trench.

To address the issue of the seam a modified process flow was developed. As shown in Figure 9, the new process deposited 1000A of oxide in the trench followed by 2000A of amorphous silicon. The silicon was then etched with an unmasked DRIE. This removed the silicon from the surface of the wafer and the bottom of the trenches, but it remained on the side walls forming a spacer. Next the oxide was etched from the bottom of the trench using an RIE process. The result of this processing is shown in Figure 10. By using this process a small foot is formed in oxide lining the trench. When the silicon is etch to form the tube, this foot makes creates a narrow space at the bottom of the trench that will seal first during the LPCVD deposition.

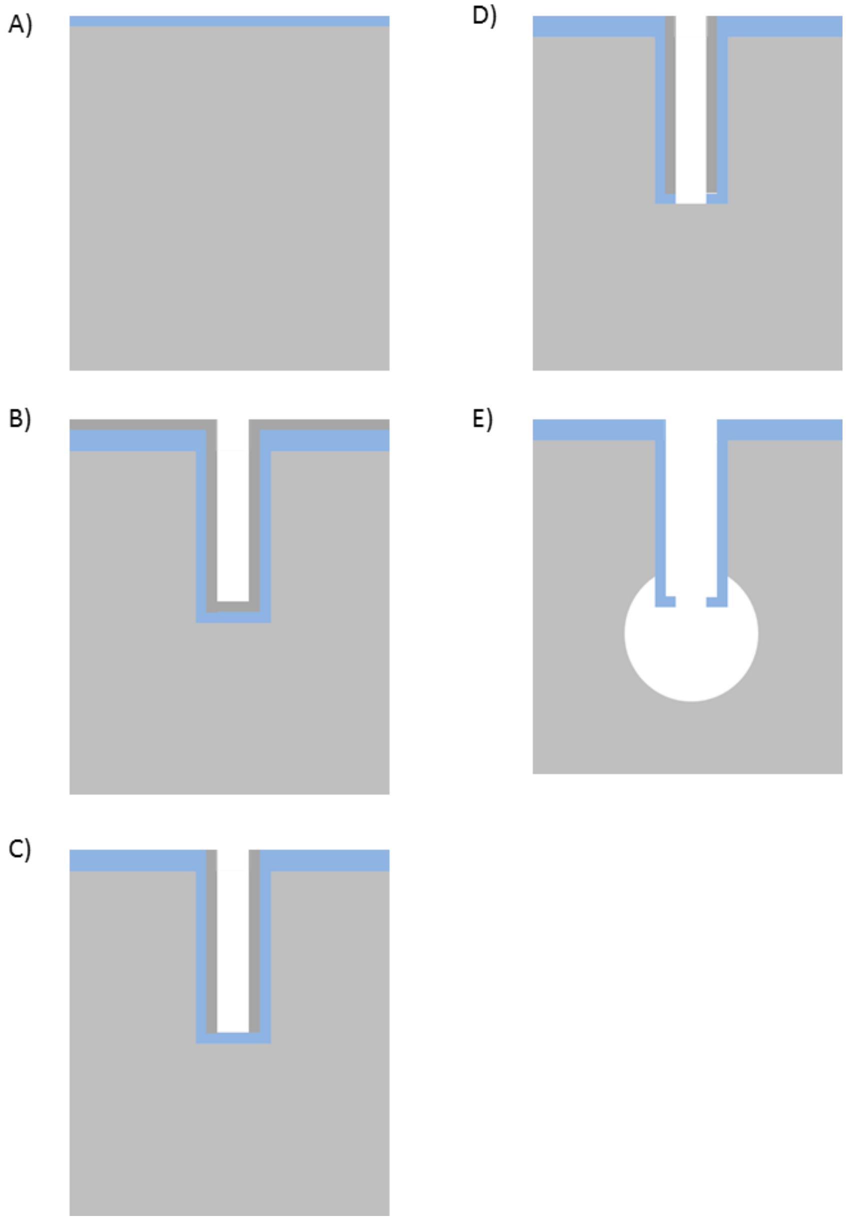

Figure 9: Revised Process flow for tube formation. A) the process begins with a silicon wafer covered with SiO2. B) DRIE is used to etch a trench, and followed by 1000A LPCVD oxide and 2000A a-Si. C) An unpatterned DRIE removes the a-Si from the bottom of the trench and the surface. D) RIE is used to remove the oxide at the bottom of the trench. E) An isotropic etch defines the tube.

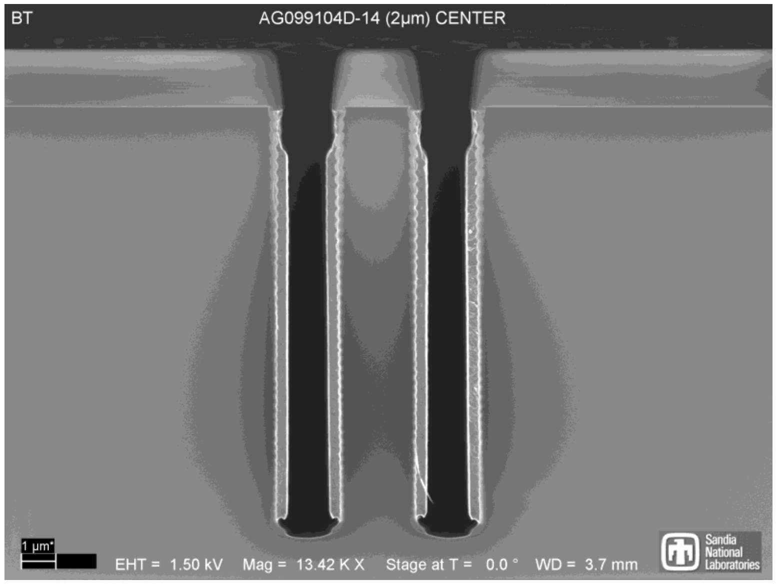

Figure 10: A 2um x 10um trench showing the a-Si spacer and the oxide foot at the bottom of the trench.

In addition to the new process flow detailed above, an experiment was performed to investigate using an inductively coupled (ICP) SF6 plasma for the silicon isotropic etch. The process was performed in an STS DRIE tool, used 450sccm of SF6, with 2000W of ICP power and 0 watts of bias power. The resulting etch profiles for various times and trench widths are shown in Figure 11 and Figure 12. At 100 seconds for etching, the profile looks isotropic. However for the smaller trench sizes, the minimum interior dimension of the tube would be less than 3um after depositing the SiN. At the time this experiment was performed, it was believed that this would be too small to carry enough gas to use as an effective cooling device. In the case of the 300 second etch, the profile obtained has a distinct heart shape. Other process variations using the STS were tried, but the result in all cases was similar to those shown below.

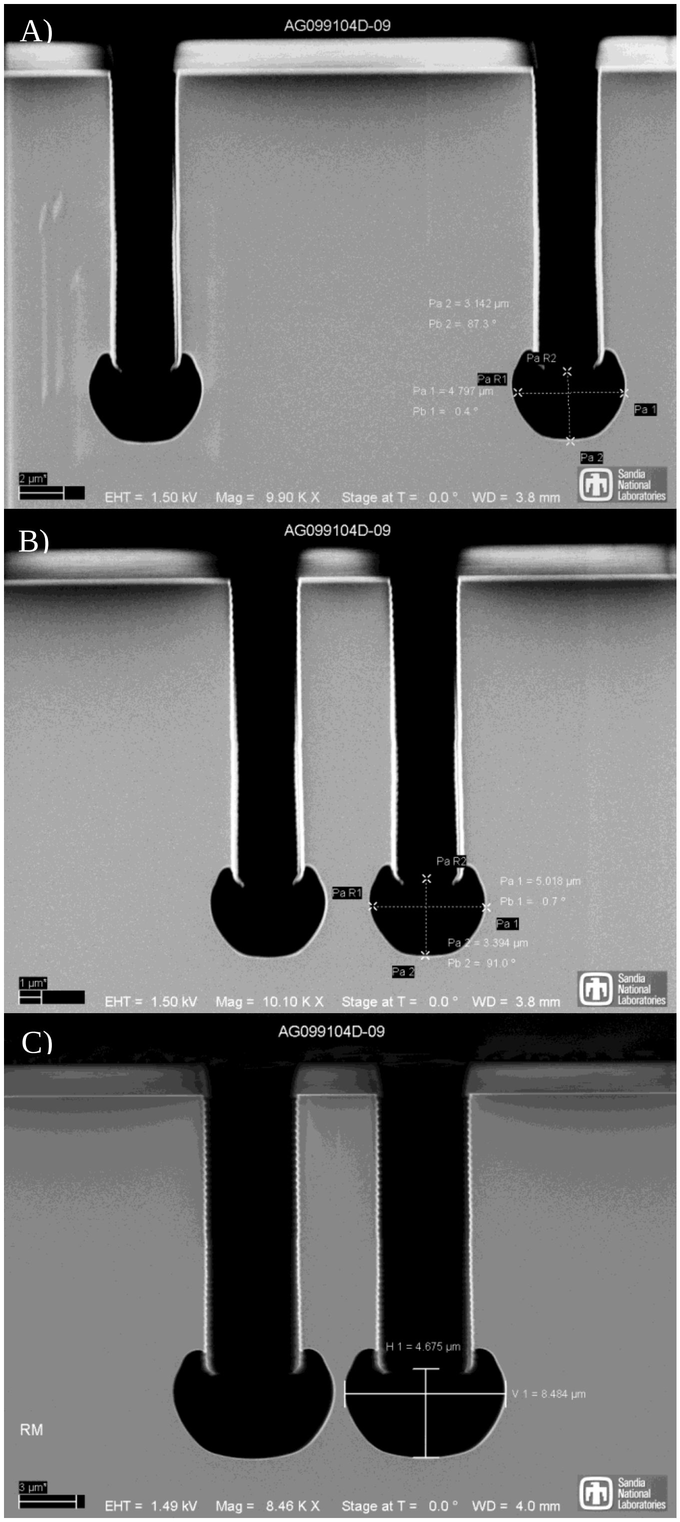

Figure 11: Cross-sections of sub-surface tubes formed using an SF6 plasma with 0 bias power for 100 seconds. For this etch time, the profile is rounder than with the CDE etches shown previously. The profiles were formed by starting with A) a 2um x10 (width x height) trench, B) a 3um x 10 um trench, and C) a 5 um x 10um trench.

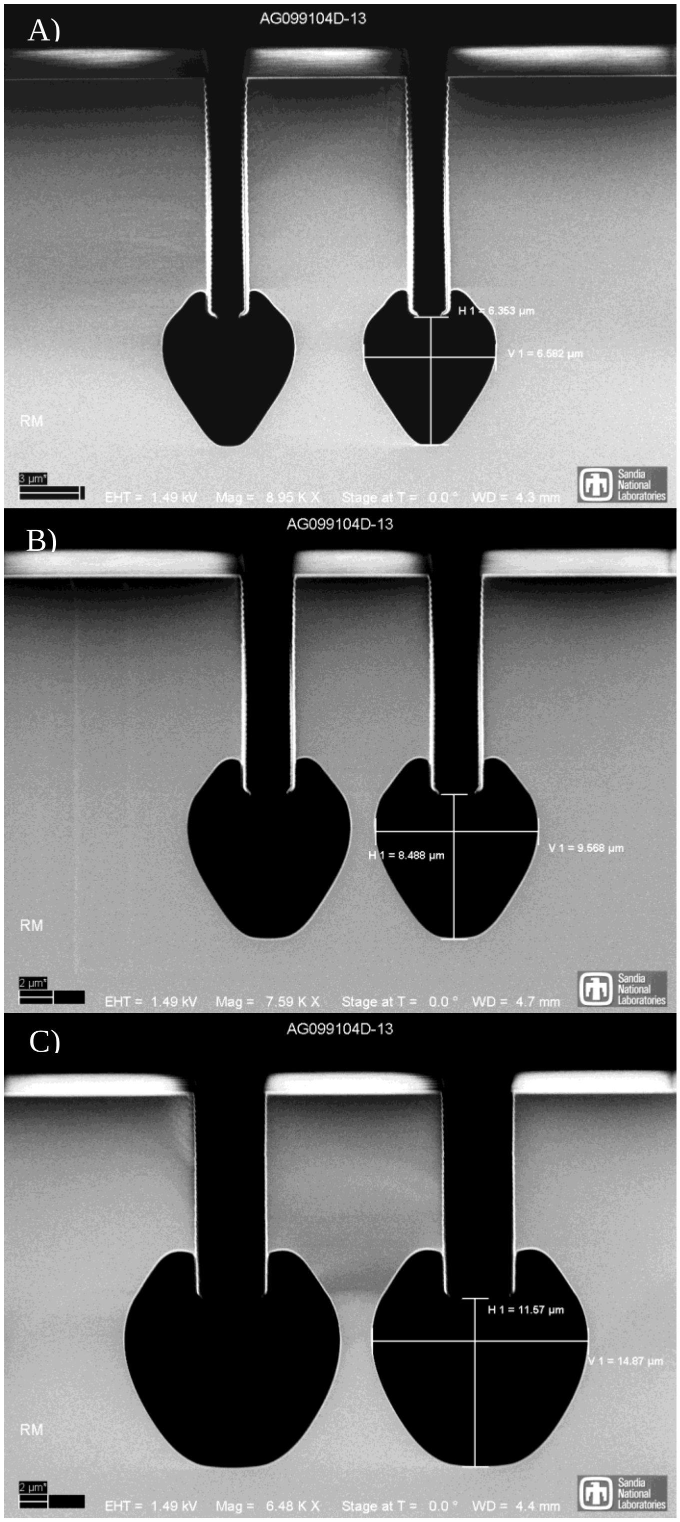

Figure 12: Cross-sections of sub-surface tubes formed using an SF6 plasma with 0 bias power for 300 seconds. For this etch time, the profile is rounder than with the CDE etches shown previously. The profiles were formed by starting with A) a 2um x 10um (width x height) trench, B) a 3um x 10 um trench, and C) a 5 um x 10um trench

3.3 Stress Simulations Of Realized Geometries

Finite element stress analysis was performed on a tube with the etch profile obtained in from the 300 second SF6 etch on the 3um trench. The simulation was performed on tubes with both 1um and 1.5 um thick SiN walls with an 80 atm interior pressure. The results indicate stress as high as 230 MPa for the 1um thick case and 120MPa for the 1.5um thick case. The stress was concentrated in the corners. Literature indicates that the fracture stress of thin film SiN is between 100MPa and 200MPa depending the film quality, meaning that these structures are likely to fail. Wall thickness greater than 1.5um would be difficult to achieve with the integration being pursued, and would result in increased thermal conduction losses. In addition, at the time simulations based on the simplistic model presented above suggested that an inner diameter of at least 4um would be needed in order to transport enough gas for effective cooling. This meant that further investigation of smaller structures with a more uniform profile was not pursued.

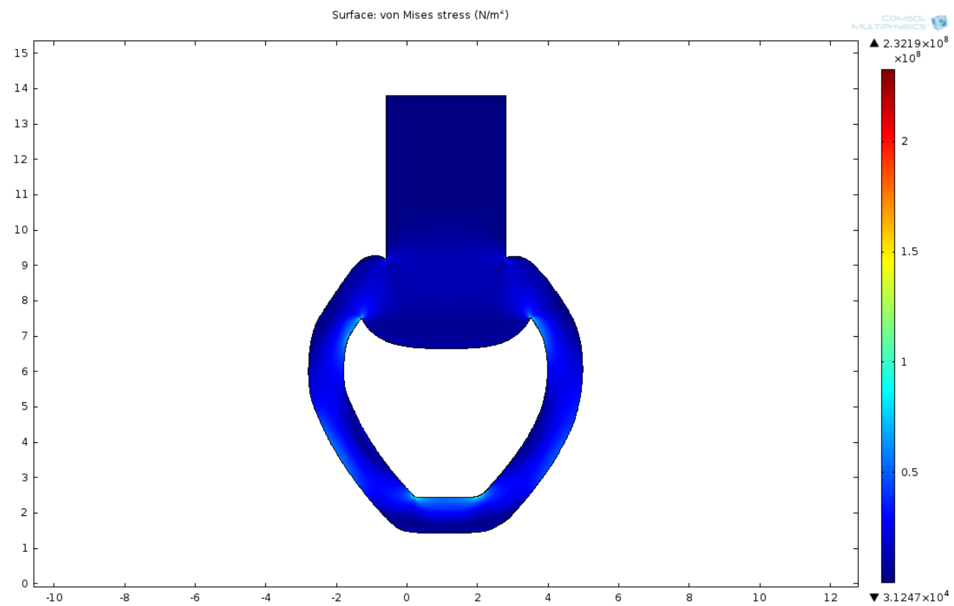

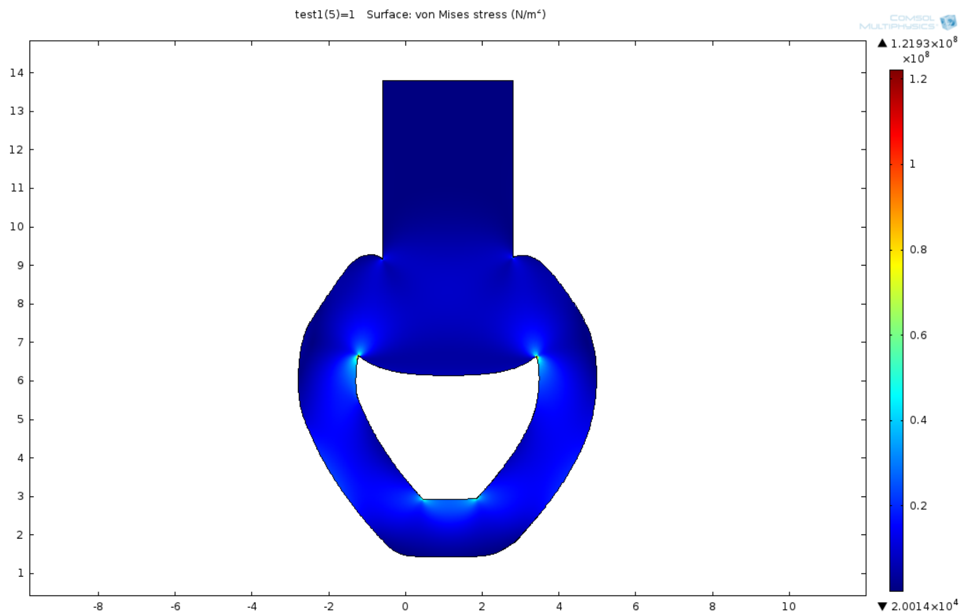

Figure 13: Stress simulations of tube profiles based on a 300 sec SF6 etch. Above with a 1um wall, below with a 1.5 um wall.

4. NUMERICAL SIMULATION OF COUNTER-FLOW HEAT EXCHANGER

4.1 Modeling Gas Expansion

Comsol was use as the finite element tool to simulate a J-T cooler. The first step of the modeling process was to demonstrate modeling of the expansion of gas, in this case nitrogen. The gas models supplied with Comsol do not specify heat capacity Cp as a function of pressure, and as a result they could not be used to model the J-T affect. Instead, an empirical gas model was supplied to the software by using the NIST webbook data[9] for nitrogen over wide range of temperatures and pressures. The software was configured to perform laminar flow, thermo-fluidic simulations on an axis-symmetric geometry, with a no-slip wall boundary condition. The geometry used for the simulations is shown in Figure 14. It consists of a 20um wide pipe, separated by a long thin channel, whose diameter was varied in the simulations. One end of the system was given a pressure boundary condition of 5 atm, while the other end was set to a pressure that was varied. The high pressure incoming gas was fixed at 300K, and the only other place heat could leave (or enter) the system was through the low pressure outlet. The notch shown in the low pressure pipe is for convenience, as it helps to reduce variation in the velocity and temperature of the gas at the outlet. This made quickly analyzing the total temperature change simpler.

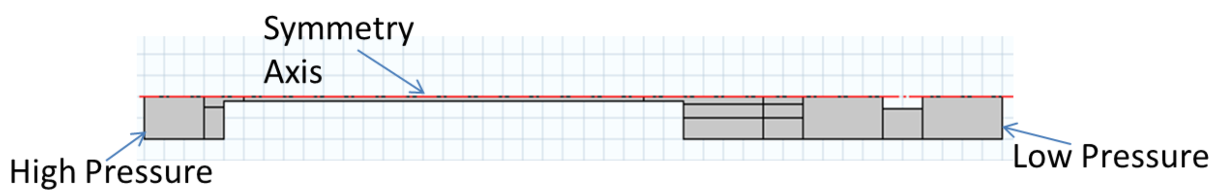

Figure 14: An example of the geometry used model free expansion of nitrogen through a restriction.

The system was simulated with a range of pressures, diameters and lengths. Figure 15 shows an example of a simulation performed using a restriction 0.7um in diameter and 175um long, with 40atm applied to the high pressure inlet, for a pressure difference of 35atm (the simulation parameter named Pin, as shown in Figure 15, was used to represent the pressure difference across the system, and not the absolute pressure.) The simulate temperature of the gas leaving the system in 292.8K, and the maximum velocity reached by the gas as it leaves the restriction is 140 m/s, as shown in detail in Figure 16. The theoretical minimum temperature that can be expected is 292.9K. The simulated mass flow through the restriction was 1.68e-8 g/s. Table 1 shows the mass-flow and exiting gas temperature for several simulated variations. There are some discrepancies between the simulated temperature and the theoretical minimum, particularly at 80atm inlet pressure. This is likely do to numerical error associated with the high velocity gradients calculated for the highest pressures. A finer mesh may produce better results, but was not tested due to RAM limitation on the simulation platform. However the general consistency of the simulated temperature over different geometries, pressures and mass-flow rates gave me confidence that this type of model could be used to simulate a complete J-T cooler, including the restriction.

Table 1: Gas flow simulation results show isenthalpic cooling at various pressures in various channel geometries

Length (um)	Diameter (um)	Pressure (atm)	Mass Flow (g/s)	Simulated Temperature (K)	Theoretical Minimum Temperature (K)
175	0.7	20	4.05E-08	297.0	296.9
		40	1.68E-07	292.8	292.9
		60	3.74E-07	288.7	289.3
		80	5.82E-07	285.4	285.7
1015	1.5	20	1.47E-07	296.9	296.9
		40	6.14E-07	292.9	292.9
		60	1.37E-06	289.1	289.3
		80	2.40E-06	284.9	285.7
1015	1.0	20	2.92E-08	297.0	296.9
		40	1.22E-07	292.9	292.9
		60	2.74E-07	289.1	289.3
		80	4.85E-07	285.2	285.7

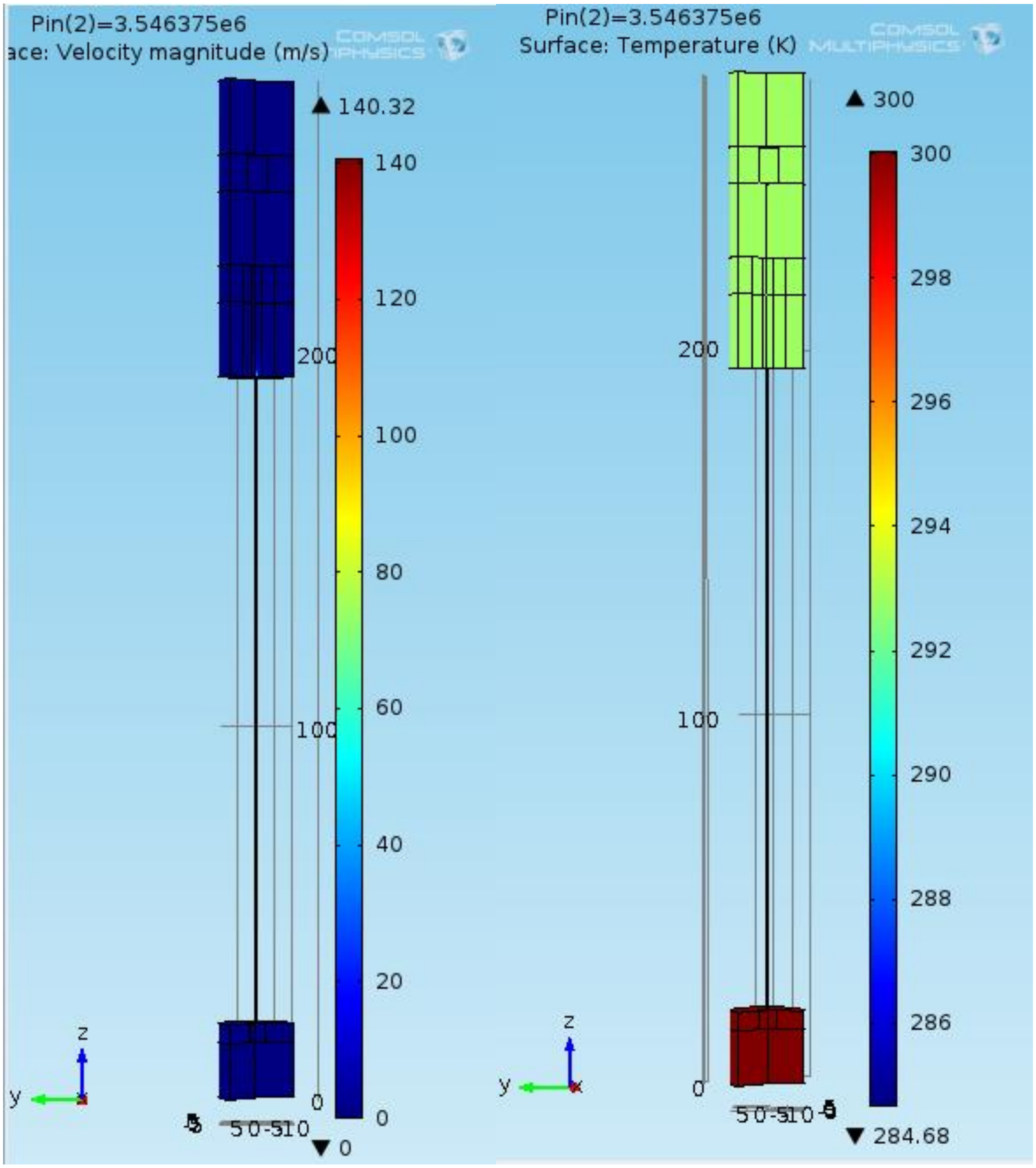

Figure 15: Left) 3-D rendering of the velocity in a thin pipe restriction. Right) 3-D rendering of the temperature profile along a thin pipe restriction.

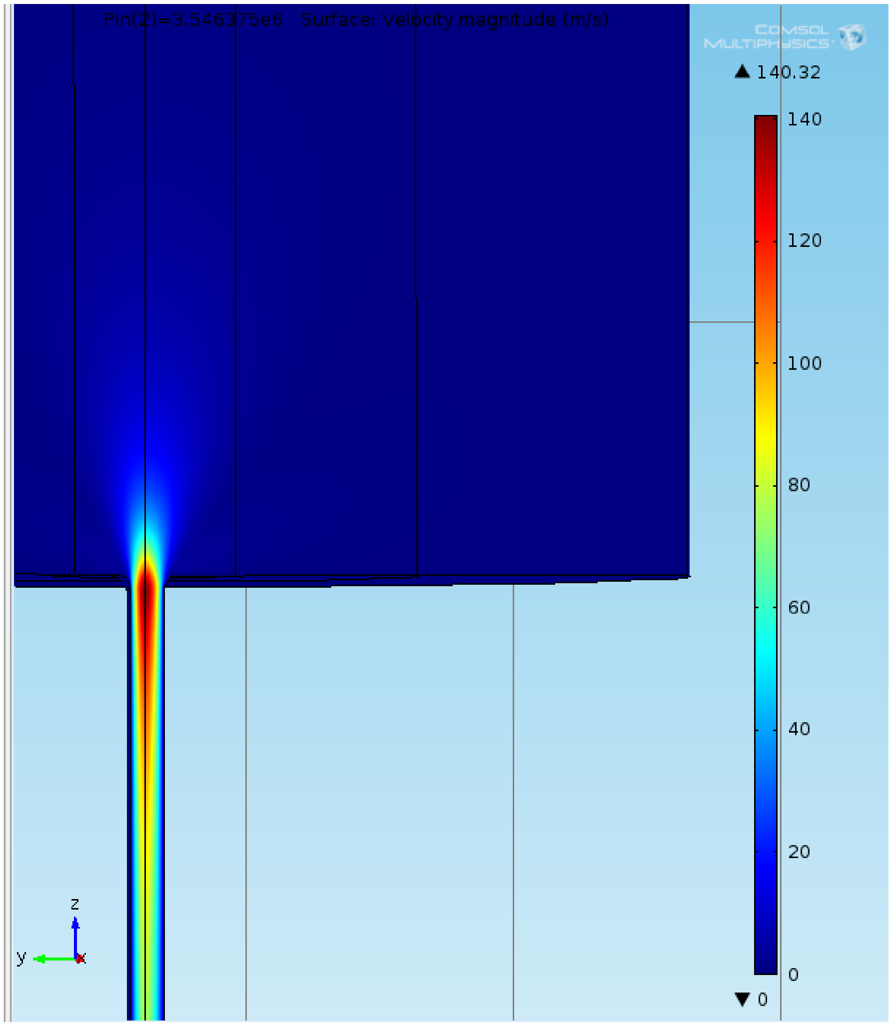

Figure 16: A close-up rendering of the simulated velocity profile at the interface between the restriction the 20um pipe at the low-pressure side.

4.2 Finite Element Analysis of a Joule-Thomson Cooler

As can be seen in Figure 16, the modeling of the restriction showed that the velocity of the gas increases dramatically near the outlet into the low pressure piping, while the velocity in the remainder of the tubing is modest by comparison. The corresponding drop in pressure is likewise concentrated at the at the low pressure end of the restriction tube, causing the system to look like a thin tube, with a restriction at the end. Simulations were performed to investigate whether this behavior could be used to create a J-T cooler that did not have a separately fabricated restriction, but instead would only use the fluidic resistance of the counter-flow heat exchanger.

Simulation was performed using a structure with the following properties:

- The diameter of the tube carrying the high pressure flow was 1.5um.
- The wall of the inner tube had a thickness of .5um and assigned the material properties of Silicon Nitride.
- The inner diameter of the return flow tubing was 2um and the outer diameter was 4um.

- The outer wall of the return flow tube was 0.5um thick and assigned the material properties of Silicon Nitride.
- The high pressure channel had a length of 1000um, and there was a 100um long cavity and the end of the narrow inner tube.
- The inlet pressure was set to 45 atm
- The outet pressure was set to 5 atm.
- The hot side of the device, and the temperature of the gas at the inlet was fixed at 300K.

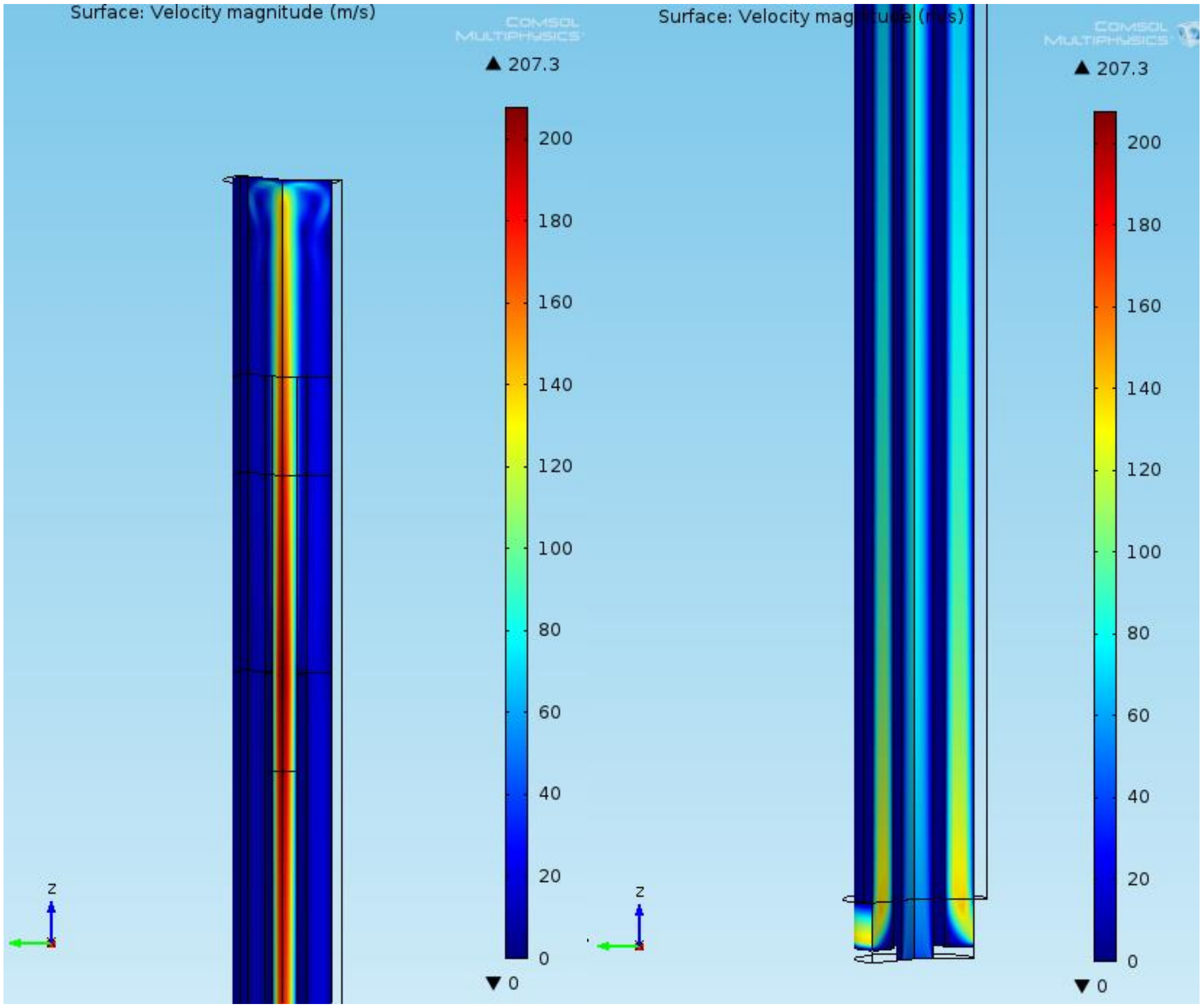

Figure 17: (Left) Simulated gas flow at the transition from the narrow high pressure tube to the wider low pressure tubing in the CFHX. (Right) Simulated gas at the outlet of the CFHX.

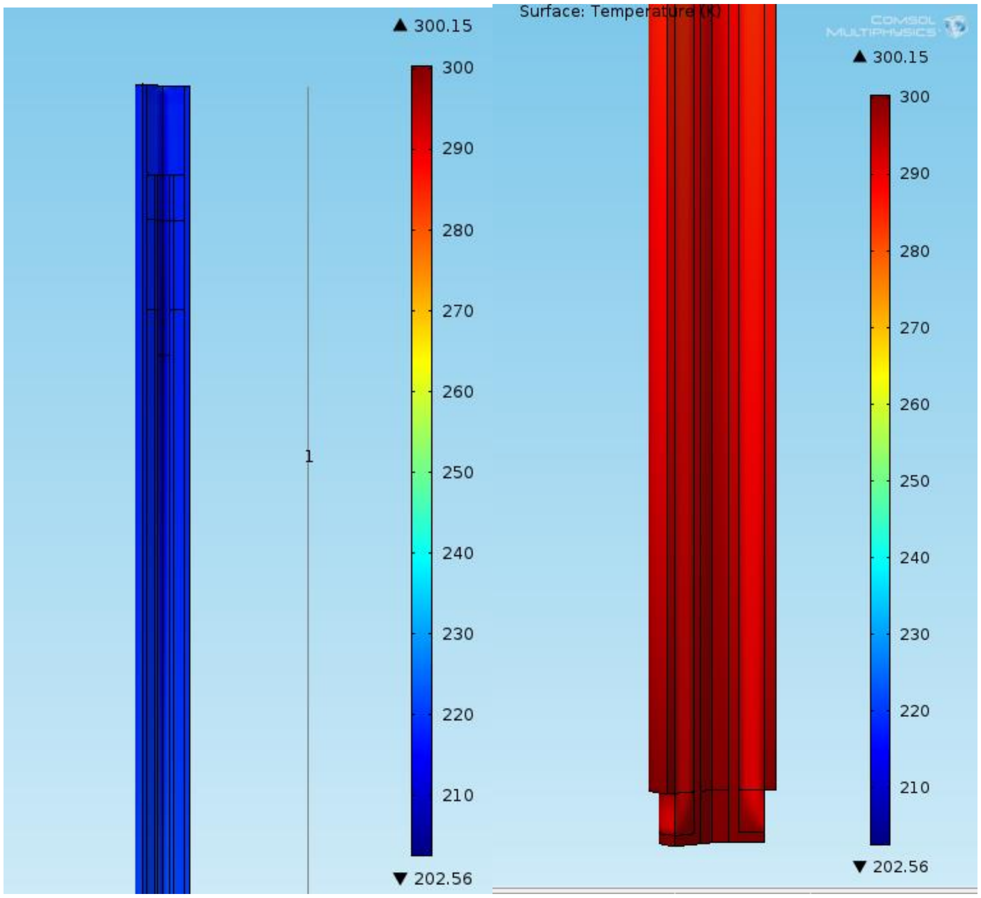

Figure 18: (Left) Simulated temperature at the cold end of the device, showing a temperature at the wall of approximately 220K. (Right) From the same simulation, the temperature at the inlet showing the 300K boundary condition used for the simulation.

Figures 17 and 18 illustrate the results of this simulation, and show that such a device would indeed act both the CFHX and the gas flow restriction at the same time. If the device was not able to operate as an effective restriction for the gas expansion, isenthalpic cooling would be minimal. Similarly, if the device was not operating at as a CFHX, the incoming gas stream would not be cooled prior to expansion, and the minimum temperature would be limited to about 290K as in the simulations presented in the previous section. The fact that the temperature of the outer wall of the device reached 220K at the cold end, indicates that both isenthalpic expansion of the gas and heat exchange between the incoming and outgoing gas flows was occurring. Due to numerical instabilities, simulations were not completed with inlet pressure in excess of 45 atm.

This result is significant for 2 reasons. First, it indicates that a co-axial structure could be used to fabricate the entire J-T cooler, without the need to fabricate a fluidic restriction external to the CFHX. Second it demonstrates that meaningful cooling levels could be achieved using low pressures, 45atm instead of 80atm, and smaller channels, 2um in diameter instead of 4um. Together, these two design criteria would result in a significant reduction in the overall stress in the tubing. In fact, contrary to the earlier assumptions, a tube fabricated using the processes discussed previous in this report might in fact be suitable for such a device. However, due to time constraints that hypothesis could not be further explored, and remains a topic for future research.

5. REFERENCES

1. Bulman, Gary E., Ed Siivola, Ryan Wiitala, Rama Venkatasubramanian, Michael Acree, and Nathan Ritz. "Three-stage thin-film superlattice thermoelectric multistage microcoolers with a ΔT max of 102 K." *Journal of electronic materials* 38, no. 7 (2009): 1510-1515.
2. Cao, H. S., P. P. P. M. Lerou, A. V. Mudaliar, H. J. Holland, J. H. Derking, D. R. Zalewski, and H. J. M. ter Brake. "Analysis of Multi-Stage Joule-Thomson Microcoolers." (2008).
3. Lerou, P. P. P. M., H. Jansen, G. C. F. Venhorst, J. F. Burger, T. T. Veenstra, H. J. Holland, H. J. M. ter Brake, M. Elwenspoek, and H. Rogalla. "Progress in Micro Joule-Thomson Cooling at Twente University." In *Cryocoolers 13*, pp. 489-496. Springer US, 2005.
4. Lin, M-H., P. E. Bradley, H-J. Wu, J. C. Booth, R. Radebaugh, and Y. C. Lee. "Design, fabrication, and assembly of a hollow-core fiber-based micro cryogenic cooler." In *Solid-State Sensors, Actuators and Microsystems Conference, 2009. TRANSDUCERS 2009. International*, pp. 1114-1117. IEEE, 2009.
5. Lerou, P. P. P. M., G. C. F. Venhorst, C. F. Berends, T. T. Veenstra, M. Blom, J. F. Burger, H. J. M. Ter Brake, and Horst Rogalla. "Fabrication of a micro cryogenic cold stage using MEMS-technology." *Journal of Micromechanics and Microengineering* 16, no. 10 (2006): 1919.
6. Zhu, Weibin. "Lithographically Micromachined Si/Glass Heat Exchangers for Joule-Thomson Coolers." PhD diss., University of Wisconsin, 2009.
7. Potkay, Joseph A., Gordon Randall Lambertus, Richard D. Sacks, and Kensall D. Wise. "A low-power pressure-and temperature-programmable micro gas chromatography column." *Microelectromechanical Systems, Journal of* 16, no. 5 (2007): 1071-1079.
8. de Boer, Meint J., R. Willem Tjerkstra, J. W. Berenschot, Henri V. Jansen, G. J. Burger, J. G. E. Gardeniers, Miko Elwenspoek, and Albert van den Berg. "Micromachining of buried micro channels in silicon." *Microelectromechanical Systems, Journal of* 9, no. 1 (2000): 94-103.
9. E.W. Lemmon, M.O. McLinden and D.G. Friend, "Thermophysical Properties of Fluid Systems" in **NIST Chemistry WebBook, NIST Standard Reference Database Number 69**, Eds. P.J. Linstrom and W.G. Mallard, National Institute of Standards and Technology, Gaithersburg MD, 20899, http://webbook.nist.gov

DISTRIBUTION

1	MS0899	Technical Library	9536 (electronic copy)
1	MS0359	D. Chavez, LDRD Office	1911

Sandia National Laboratories